infrastructures

MDPI

Article

Alkali-Silica Reaction Resistance and Pore Solution Composition of Low-Calcium Fly Ash-Based Geopolymer Concrete

Jiawei Lei, Jiajun Fu and En-Hua Yang *

School of Civil and Environmental Engineering, Nanyang Technological University, 50 Nanyang Avenue, Singapore 639798, Singapore; LEIJ0003@e.ntu.edu.sg (J.L.); FUJI0011@e.ntu.edu.sg (J.F.)

* Correspondence: ehyang@ntu.edu.sg; Tel.: +65-6790-5291

Received: 14 October 2020; Accepted: 4 November 2020; Published: 6 November 2020

Abstract: Low-calcium fly ash-based geopolymer concrete is generally reported to be less vulnerable to alkali-silica reaction (ASR) than conventional ordinary Portland cement concrete. However, the lack of understanding of pore solution composition of the low-calcium fly ash-based geopolymer limits the investigation of the underlying mechanisms for the low ASR-induced expansion in the geopolymer concrete. This study presents a systematic investigation of the pore solution composition of a low-calcium fly ash-based geopolymer over a period of one year. The results show that the pore solution of the fly ash geopolymer is mainly composed of alkali ions, silicates, and aluminosilicates species. The lower expansion of the geopolymer concrete in the current study is most probably due to the insufficient alkalinity in the geopolymer pore solution as the hydroxide ions are largely consumed for the fly ash dissolution.

Keywords: alkali-silica reaction; geopolymer; pore solution; pH; durability; fly ash

1. Introduction

Alkali-silica reaction (ASR) is one of the major durability issues in ordinary Portland cement (OPC) concrete, which was firstly identified as a cause of concrete deterioration since 1940 [1]. The reaction occurs when the reactive form of silica in aggregates is attacked and dissolved by the hydroxyl ions in the alkaline pore solution in the OPC matrix. ASR could result in expansion, cracking, and even disruption of the OPC concrete structures [2,3]. Using sufficient quantities of supplementary cementitious materials (SCM) is one of the most common means of controlling ASR in OPC concrete [4]. While the appropriate SCM dosage in a concrete to mitigate ASR has to be determined by the ASR testing case by case [5], as the SCM content required to control ASR varies widely depending on the nature of the SCM, the aggregates reactivity, the availability of the alkalis within the concrete and the exposure conditions of the concrete [6]. It should also be cautious that high substitution levels of OPC with SCM can adversely affect other concrete properties, i.e., strength development, setting, and freeze–thaw resistance [4].

Fly ash-based geopolymer is a cementitious binder produced by the activation of the fly ash with low-CaO content (ASTM Class F) by a highly concentrated alkaline solution [7]. It has gained intense research interests as promising alternative binders to OPC due to their comparable mechanical and rheological property in the hardened and the fresh states, respectively, but with reduced environmental footprint and superior durability in contrast to OPC [8,9]. Studies [10–13] on the ASR-behavior of the low-calcium fly ash-based geopolymer concrete in the presence of reactive aggregates consistently showed that the ASR-induced expansion in the geopolymer concrete was substantially smaller than that of the OPC concrete in laboratory investigations, indicating the low-calcium fly ash-based geopolymer concrete is more resistant to ASR than the conventional OPC concrete.

The differences in the pore solution composition between fly ash-based geopolymer and OPC paste could be the potential reasons for the low ASR expansion of the geopolymer concrete since the pore solution composition directly influences the ASR process and the gel expansion according to the studies on ASR in OPC system [4,14]. Specifically, it has been shown that sufficient alkalinity in the pore solution is essential for the reactive silica to be attacked at a certain rate that will lead to deleterious ASR expansion [4,15]. Moreover, the calcium hydroxides from the hydration of tri- and di-calcium silicates in OPC act as a large reservoir of hydroxide ions to maintain the pH level of the pore solution, which ensures the continuation of the ASR in OPC concrete [16]. It has also been suggested that calcium could facilitate the gelation process [17,18] and modify the physical and chemical properties of the ASR gel [19,20] in OPC concrete. The shortage of calcium may lead to the formation of gel with low expansion pressure [19] or even no gel formation [21]. Furthermore, it was reported that the presence of soluble aluminum in the pore solution of blended OPC concrete was able to significantly reduce the ASR expansion of the concrete [21–23]. It was suggested that the effects of aluminum were probably attributed to the incorporation of aluminum into the reactive silica surface, resulting in a reduction of the silica dissolution rate [22]. Therefore, the variations of the alkali, calcium and aluminum content in the pore solution of the fly ash-based geopolymer are the critical factors influencing the ASR resistance of the geopolymer concrete.

The significant role of pore solution in ASR has led to extensive investigations of pore solution composition in OPC paste and mortar [16], however, the composition of the pore solution in the low-calcium fly ash-based geopolymer paste has been rarely studied. The lack of understanding of the pore solution composition of the low-calcium fly ash-based geopolymer limits further investigations on the underlying mechanisms governing the ASR resistance of the geopolymer concrete.

In previous studies [10–13], the ASR-behavior of the low-calcium fly ash-based geopolymer was investigated by using the accelerated mortar bar test (AMBT) according to ASTM C1260 [24]. During the test, mortar bars samples were immersed in 1 mol/L NaOH solution at 80 °C. The severe test condition is applied to accelerate the ASR in OPC mortar bars, while this aggressive condition was reported to influence the chemical stability of the fly ash geopolymer matrix. The external alkali source and the elevated temperature that the mortar bars experience in AMBT may continue to activate the unreacted fly ash within the mortar bars [10] and could also lead to the formation of zeolitic phases in the storage solution and the mortar specimens [11,12,25], which makes the applicability of this method to fly ash-based geopolymer mortar questionable. The concrete prism test (CPT), ASTM C1293 [26], which is currently considered as the most representative ASR test method in laboratory investigations when compared to structures in actual field conditions [27], may be more suitable to evaluate the ASR-behavior of the fly ash-based geopolymer concrete as the specimens are not immersed into NaOH solution and the temperature is closer to ambient temperature.

This study thus strived to systematically investigate the pore solution composition in a low-calcium fly ash-based geopolymer over a period of one year, which could provide information for the analysis on the ASR-behavior of the geopolymer concrete. The ASR expansion behavior was evaluated according to the concrete prism test (CPT), ASTM C1293 [26]. The pore solution of the corresponding fly ash geopolymer pastes with varied ages was extracted and analyzed to show the variations of the geopolymer pore solution over one year, based on which, its potential influences on the ASR-behavior of the low-calcium fly ash-based geopolymer concrete were illustrated.

2. Materials and Methods

2.1. Materials

The class F fly ash with compositions shown in Table 1 was used for geopolymer synthesis. Silica and alumina constitute 58.6% and 30.4% by mass, respectively, of the fly ash. Activating solution of sodium hydroxide with concentration of 10 mol/L was prepared by dissolving NaOH pellets (AR grade, purity ≥ 99%) into deionized water. After full dissolution, the solution was cooled down for 24 h

to room temperature before geopolymer synthesis. Type I Portland cement with Na2Oeq of 0.66% (Table 1) was used for the OPC specimens. The alkali-silica reactive aggregates used in this work are the local sedimentary rocks extracted from Jurong Rock Caverns, Singapore. The main crystal phases of the rocks are quartz and albite [28].

Table 1. Chemical compositions of the raw materials (% by mass).

	SiO_2	Al_2O_3	Fe_2O_3	CaO	MgO	K_2O	Na_2O	P_2O_5	SO_3	TiO_2
Cement	17.6	3.2	3.1	62.5	3.6	0.4	0.4	0.1	3.6	0.6
Fly ash	58.6	30.4	4.7	1.2	0.8	1.5	-	0.5	0.1	2.0
Reactive aggregates	63.7	13.3	3.8	2.2	0.5	4.1	3.5	0.1	2.1	0.4

2.2. Methods

2.2.1. Concrete Prism Test (CPT)

The OPC concrete prisms with dimensions of 75 mm × 75 mm × 285 mm and a water-to-cement ratio of 0.45 were prepared in accordance with ASTM C1293. NaOH pellets were dissolved into the mixing water to increase the alkali content of the OPC to 1.25% Na_2Oeq. The fly ash geopolymer concrete prisms were prepared in the same procedure only except that the cement was replaced by fly ash and the mixing water was replaced by the 10 mol/L NaOH activating solution. While silicates are usually contained in alkaline activators to control the composition of fly ash geopolymer, only NaOH solution is used as the activator in the present work for simplicity. The local ASR reactive aggregates with fineness modulus of 4.54 and grading shown in Figure 1 were used in both the OPC and the geopolymer concrete prisms with an aggregate-to-binder ratio of 2.3, by mass.

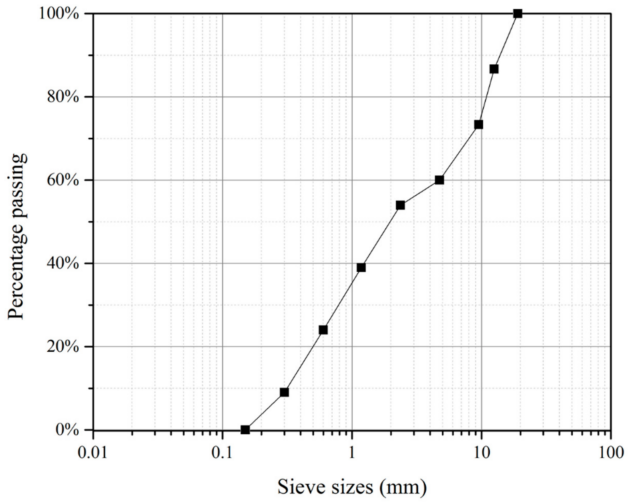

Figure 1. Grading curve of the reactive aggregates.

After casting, the OPC concrete prisms were cured at 23 °C for 24 h and the fly ash geopolymer concrete prisms were cured at 80 °C for the same duration (i.e., 24 h), which is commonly applied for fly ash-based geopolymer to facilitate the polymerization in the early age due to the relatively low reactivity of fly ash. All the specimens were cured in an environmental chamber with 98% RH to prevent moisture loss. After curing for 24 h, the prisms were de-molded and stored over water in a sealed container. The absorbent material made of polypropylene geotextile was attached to the inner sides of the container from the top into the water at the bottom. The container was then placed in an oven at 38 °C. The lengths of the specimens were measured routinely for 12 months and the average expansion readings of three prisms for each type of specimen together with its standard deviation were reported.

Optical and electron microscopic analyses were carried out on the prism specimens after the test. Thin section samples with a thickness of about 20 μm were prepared for optical microscopy by using a polarized light microscope (Olympus BX51). After that, secondary electron (SE) imaging and energy-dispersive X-ray spectroscopy (EDX) analysis were conducted on the same sample by using a field emission scanning electron microscope (FESEM, JEOL JSM-7600F). The specimens were freeze-dried under vacuum for 72 h and coated with a platinum layer to prevent charging before the SEM/EDX analysis.

2.2.2. Pore Solution Composition of Low-Calcium Fly Ash-Based Geopolymer

Geopolymer paste specimens with a diameter of 45 mm and a height of 85 mm were prepared for the pore solution extraction. The paste has the same mix design as the geopolymer concrete used in the CPT, except that aggregates were omitted in preparing the paste sample. The geopolymer paste specimens were then stored in the same condition as specified in the CPT. The pore solution of the geopolymer pastes at different ages was extracted following the method described by Barneyback and Diamond [29] by using a high-pressure extraction setup which is similar to that described by Cyr et al. [30]. An additional air circulation system was equipped to the setup to drive the extracted solution into the collection bottle and the CO_2 in the circulating air was removed by aerating it through 1 mol/L NaOH solution in order to minimize carbonation of pore solution during the extraction process. The extraction was conducted on a 3000 kN servo-hydraulic compression testing machine (MTS YAW-3000L) with a loading rate of 1.2 kN/s and loaded up to 1200 kN.

Immediately after the extraction, the pore solution was filtered by using a syringe filter with pore sizes of 0.45 μm to remove particles in the solution. After that, the pH of the solution was measured using a standard pH meter (Mettler Toledo SevenCompact) and the ion concentrations of Na, K, Si, Al, and Ca in the solution diluted into 100 times were measured by using inductively coupled plasma-optical emission spectrometry (ICP-OES, PerkinElmer Optima 8000).

In addition, the solution was analyzed by Fourier transform infrared spectroscopy (FTIR, PerkinElmer Spectrum) and solution-state nuclear magnetic resonance (NMR, Bruker Avance 400 MHz). FTIR spectra were obtained from 4000 to 400 cm^{-1} in attenuated total reflectance (ATR) mode. ^{29}Si NMR spectra were obtained at 79.49 MHz by using 90° pulses of 14.5 μs and 5-s recycle delays with a number of scans of 256. ^{27}Al spectra were obtained at 104.26 MHz by using 90° pulses of 10 μs and 1-s recycle delays with a number of scans of 64. All the spectra were obtained under the same condition at ambient temperature on 400 μL of pore solution sample with 10% of $^{2}H_2O$ for NMR locking. Chemical shifts of ^{29}Si and ^{27}Al were reported in parts per million referenced to tetraethoxysilane and $AlCl_3$ solution, respectively.

3. Results and Discussion

3.1. Concrete Prism Test (CPT)

Expansion results of the OPC and fly ash geopolymer concrete (FA) prisms are shown in Figure 2. The dash line in the figure represents the acceptable expansion limit of 0.04% at one year as prescribed in ASTM C1293. As can be seen, the OPC concrete prisms showed a rapid expansion within the first two months and continued expanding afterward with a lower expansion rate. The average expansion of OPC prisms exceeded the one-year expansion limit in 9 months, reaching 0.06% in one year. While the fly ash geopolymer prisms showed almost no signs of expansion (0.006%) after 12 months, suggesting the better resistance of the fly ash-based geopolymer concrete to ASR, which is consistent with the AMBT results in the published literature [10–13].

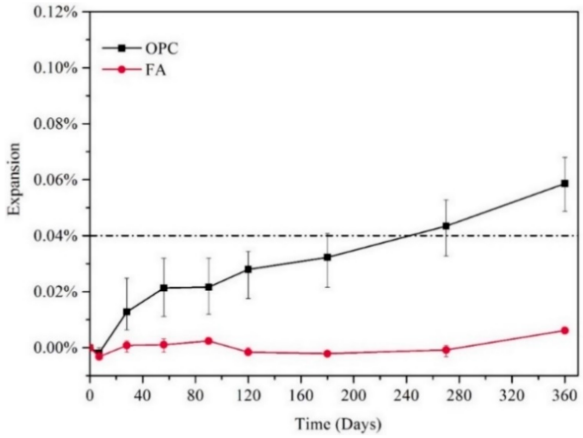

Figure 2. Expansion results of ordinary Portland cement (OPC) and fly ash geopolymer concrete prisms in concrete prism test (CPT).

In general, numerous microcracks were observed along the aggregate-matrix interfaces and extended through aggregates in the OPC concrete prism specimens after 1-year CPT. Figure 3a shows the typical polarized light microscopic images of the OPC concrete prism specimens after 1-year CPT. As can be seen, a layer of gel-like phase with thickness around 10 μm was observed at the interface between an aggregate and surrounding OPC paste matrix, and a microcrack (about 10 μm) filled with gel extending from the interface and cut through several aggregates. The SE image on the same location (Figure 3b) showed the morphology of the gel-like phase and the average chemical composition determined by EDX confirmed it is a typical ASR product with $(Na_2O + K_2O)/SiO_2$ molar ratio of 0.15 and $(CaO + MgO)/SiO_2$ molar ratio of 0.33 [31].

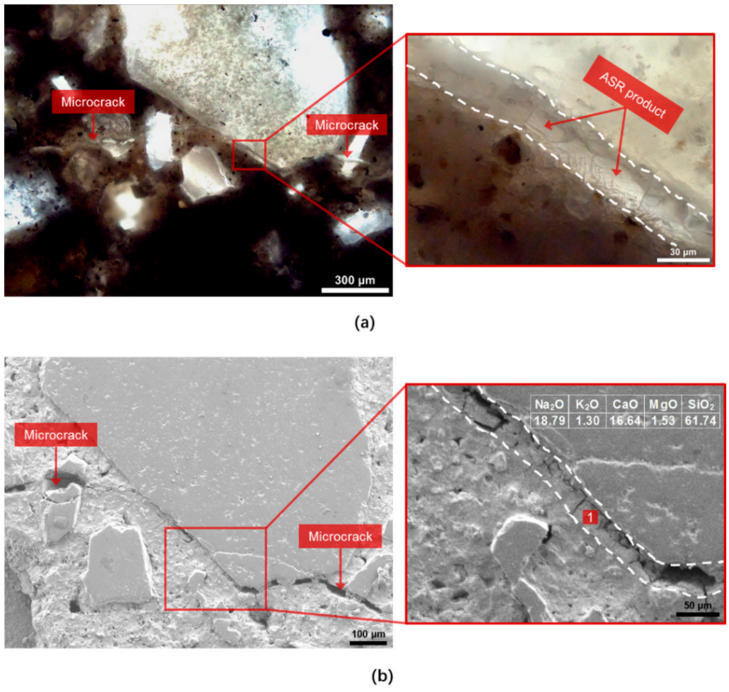

Figure 3. (**a**) Typical polarized light microscopic image of the microcracks and alkali-silica reaction (ASR) products formed in the OPC concrete prism specimens after 1-year CPT. (**b**) Secondary electron (SE) image on the same location with chemical composition (wt. %) of ASR product (site 1).

Figure 4 illustrates the typical SE image of aggregate-matrix interface of the fly ash geopolymer concrete prism specimens after 1-year CPT. Generally, no typical morphology of ASR product was observed in geopolymer concrete prism specimens and good bonding between the reactive aggregates and the surrounding geopolymer paste matrix was observed without additional phases at the interface. Few tiny microcracks (less than 1 μm) were observed in the geopolymer matrix, which were most likely introduced due to sample preparation.

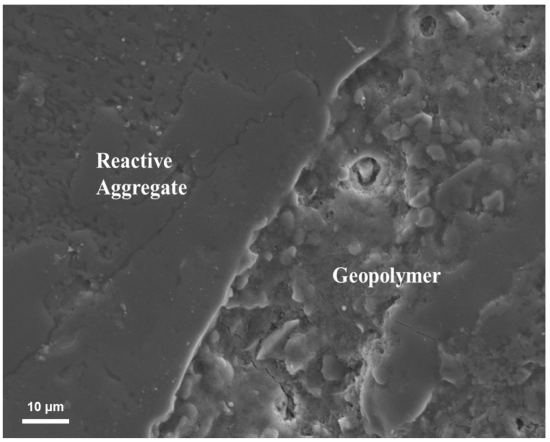

Figure 4. Typical SE image of aggregate-matrix interface of the fly ash geopolymer concrete prism specimens after 1-year CPT.

3.2. *Pore Solution Composition of Low-Calcium Fly Ash-Based Geopolymer*

The pore solution of the fly ash geopolymer paste samples with the same mix design as the fly ash geopolymer concrete prisms and stored in the same condition as specified in the CPT was extracted and analyzed. The concentrations of major ions (Na, K, Si, Al, Ca) and the pH value of the pore solution in the fly ash geopolymer paste at different ages were plotted in Figure 5. The pore solution results of fresh paste were also obtained from the extraction of the fluid paste immediately after mixing, indicated as hollow markers in Figure 5.

As can be seen in Figure 5a, the sodium concentration with a high initial value of 9.4 mol/L immediately after the mixing reduced rapidly within the first day, continued to reduce gradually in the following 6 months, and stabilized afterward at around 1.6–2.0 mol/L. The reduction of sodium content was most likely due to the participation of sodium into the geopolymer frameworks and parts of them were involved to balance the negative charge on the tetrahedral aluminum [32]. Unlike sodium ions that were mainly from activating solutions, the other ions (K, Si, Al, Ca) in the pore solution were released from the dissolution of the fly ash. Their concentrations kept increasing initially, indicating that the dissolution of fly ash was dominant in the first 7 days to provide soluble silicate and aluminate species into the solution. Then the dissolution rate gradually reduced with time and the condensation was dominant to form geopolymer gel reducing the soluble species. The concentrations of the ion species (Na, K, Si, Al, Ca) in the pore solution maintained stable after 6 months, indicating the completion of the polymerization process and the pore solution was at equilibrium with the geopolymer binders.

The pH value of the pore solution is shown in Figure 5d. As can be seen, the pH value reduced significantly from 13.8 to 12.6 in only one day and stabilized afterward. This remarkable reduction in the first day is mainly due to the rapid dissolution of fly ash in the activating solution with high alkalinity and accelerated in the curing condition at 80 °C. The hydroxide ions in the activating solution were largely consumed in the dissolution process to rapture the Si-O-Si and Si-O-Al bonds in the fly ash [33].

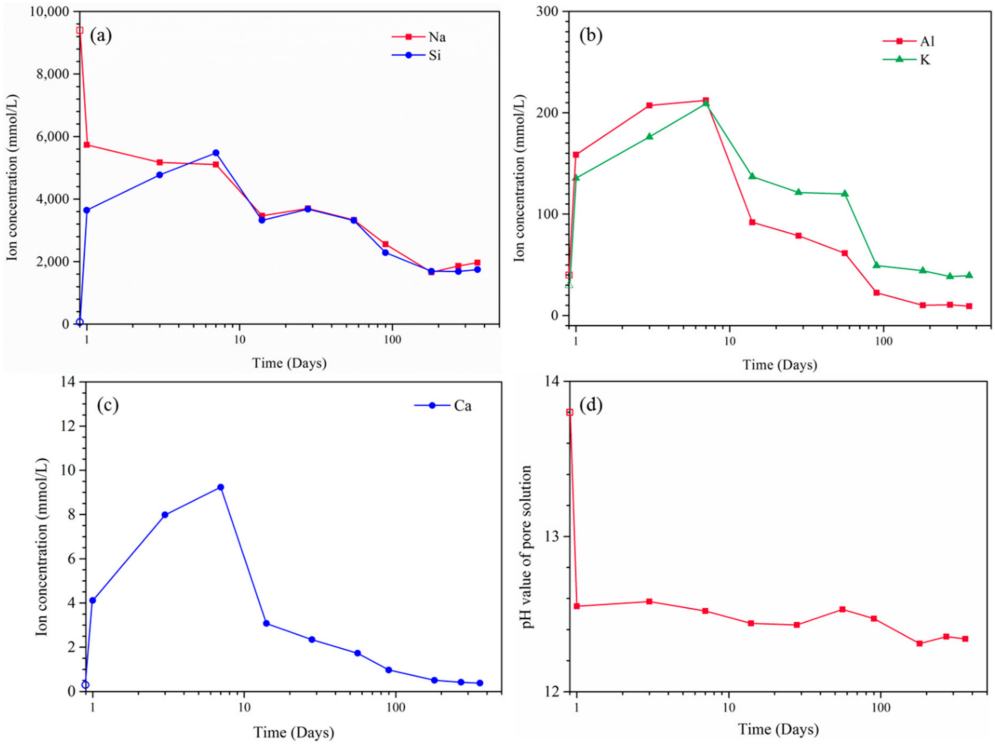

Figure 5. The concentrations of (**a**) Na, Si, (**b**) Al, K and (**c**) Ca in the pore solution as a function of time. (**d**) The pH of the pore solution as a function of time. Hollow markers are the results of the fresh paste.

Figure 6 shows the infrared spectrum between 2000 and 800 cm^{-1} for pore solution extracted from geopolymer paste specimens at ages between 1 day and 1 year. Significant bands at 1637 cm^{-1} are associated with the bending vibration of H-O-H in water molecules [34]. Major bands at 993–1003 cm^{-1} are corresponding to the asymmetric stretching vibration of Si-O-T bonds, where T is tetrahedral silicon or aluminum [34], indicating the presence of silicon or aluminum tetrahedra in connected units. The shoulder at 1100 cm^{-1} is assigned to the asymmetric stretch of Si-O-Si bonds in a relatively pure silicate phase without the incorporation of aluminum tetrahedra [35]. A slight band shift is observed from 993 cm^{-1} gradually to 1003 cm^{-1} with the increase of the sample age, most probably due to the reduced amount of aluminum, leading the peak shift to higher wavenumbers [35].

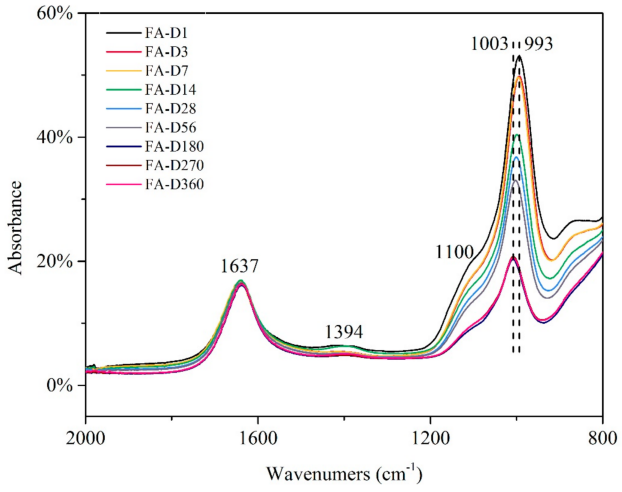

Figure 6. Fourier transform infrared spectra (800–2000 cm^{-1}) of the geopolymer pore solutions at ages between 1 day and 1 year.

The vibration band at 1394 cm^{-1} is associated with the stretching vibration of O-C-O bonds in the carbonate group [34]. Very weak vibration is observed at 1394 cm^{-1} only for the pore solution at 1 and 14 days and no obvious peak is present for the pore solution at other ages. It suggests that the carbonation on the geopolymer pore solution in the presented curing condition was very limited and the slight carbonation on the 1-day and 14-day pore solutions most probably occurred during the extraction process.

Further information on the short-range order of the aluminum and silicon in the pore solution is given by the solution-state NMR spectroscopy. The ^{27}Al NMR spectra of the geopolymer pore solutions at ages between 1 day and 1 year are shown in Figure 7. As can be seen, all spectra reveal a broad and asymmetrical band with a range of 45–80 ppm, indicating all the aluminum were tetrahedrally coordinated in the solutions [36]. The line-broadening of ^{27}Al NMR spectra is always observed due to the second-order quadrupolar line shifts [37]. The asymmetrical band indicates it consists of signals at least from two environments. Thus, a deconvolution of the ^{27}Al NMR spectra was conducted based on the peak assignments of the q^n site aluminum in the previous NMR studies on alkali aluminosilicate solutions [38,39], where q refers to tetrahedrally coordinated aluminum and the superscripts indicate the number of bridges to silicon. The spectra were fitted by Gaussian–Lorentzian Sum function with about 50% Gaussian shape. Throughout the deconvolution process peak positions and widths for each identified species were maintained constant.

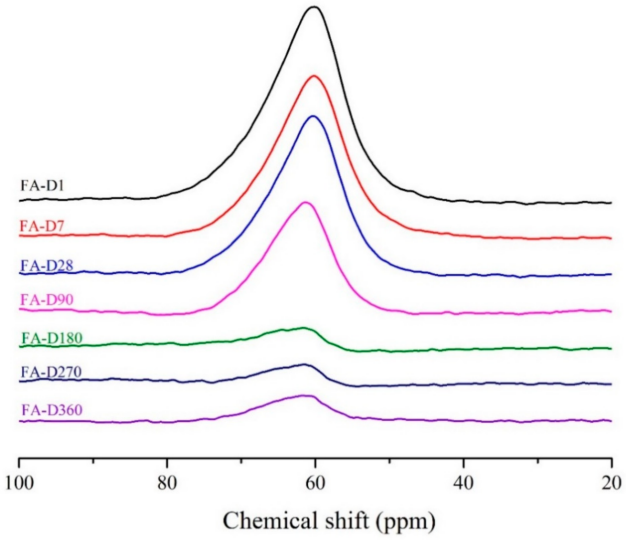

Figure 7. ^{27}Al nuclear magnetic resonance (NMR) spectra of the geopolymer pore solutions at ages between 1 day and 1 year.

The deconvolution results of the pore solution at day 1 is shown in Figure 8 and a summary of the deconvolution results are presented in Table 2. It shows that all the spectra consist of three bands, i.e., q^4, q^3, and q^2, indicating the aluminum tetrahedra are bonded with silicones and are present in aluminosilicate oligomers. The monomeric $Al(OH)_4^-$ (q^0) is reported as the predominant aluminate species in the dissolution process. However, no signal of q^0 was detected at the chemical shift of 80 ppm [40] in pore solution at all ages, suggesting the monomeric $Al(OH)_4^-$ was incorporated into aluminosilicate oligomers after dissolution within 1 day. It has been reported that $Al(OH)_4^-$ monomers are more readily to combine with long-chain silicate oligomers rather than silicate monomers [41], which agrees with the observations here that q^1 sites were absent and q^4 sites were the majority in the solution at early ages followed by q^3 sites (Table 2). The variation of the amounts of the q^4 sites Al (Figure 9) agrees well with the variation of the silicon and aluminum concentration in the pore solutions discussed earlier (Figure 5), both of which are governed by the kinetics of the dissolution-condensation in the geopolymerization process. The amounts of the q^4 sites Al slightly increased from day 1 to day

7 due to the aluminum liberated from the dissolved fly ash incorporated into the silicate oligomers. After that, the condensation of the aluminosilicates dominated, leading to the reduction of the q^4 sites. An equilibrium state was reached within the pore solution after 6 months.

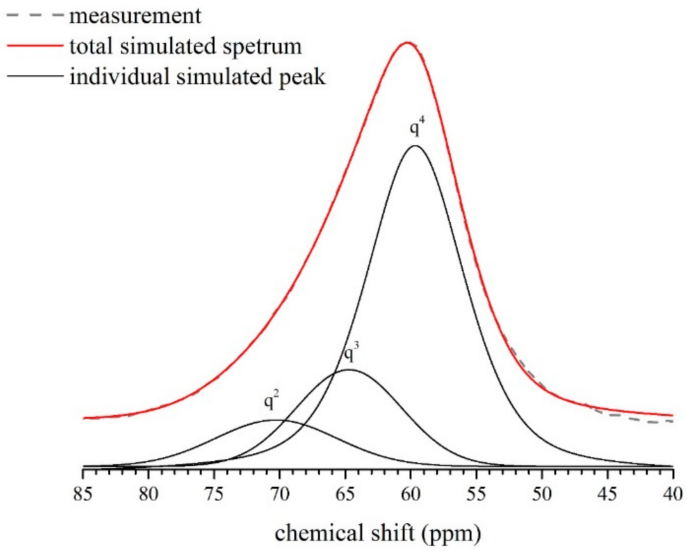

Figure 8. Deconvolution of the ^{27}Al NMR spectra of the pore solution with age of 1 day.

Table 2. ^{27}Al NMR chemical shifts and relative integrated intensities of q^n site Al from deconvolution of the ^{27}Al NMR spectra for pore solution.

Samples	Relative Integrated Peak Intensities, %		
	q^4 (59.7 ppm)	q^3 (64.7 ppm)	q^2 (70.3 ppm)
D1	72.0	18.0	10.0
D7	78.5	16.9	4.6
D28	70.4	22.9	6.7
D90	68.5	22.8	8.7
D180	45.6	43.6	10.8
D270	45.0	46.0	9.0
D360	46.2	41.9	11.9

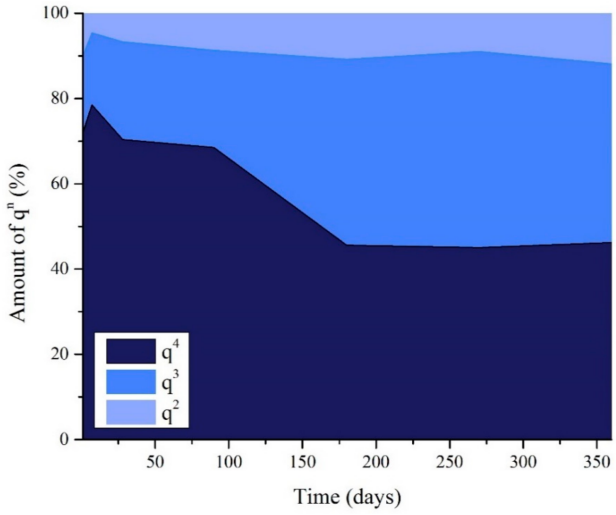

Figure 9. Amount of q^2, q^3 and q^4 sites aluminum present in the pore solution at ages between 1 day and 1 year.

^{29}Si NMR spectra of the geopolymer pore solutions at ages between 1 day and 1 year are shown in Figure 10. All the spectra consist of six distinct bands which can be assigned to Q^0, Q^1, Q^2_Δ, Q^2 and Q^3 sites silicon as indicated in Figure 10 [42], where Q refers to tetrahedrally coordinated silicon, the superscripts represent the number of siloxane bridges, and the subscript Δ designates the silicon in three-membered rings. These are the typical features commonly observed in the spectra of alkali silicate solutions [42]. The observed line boarding of the peaks is attributed to the high viscosity of the solution, which makes it difficult to distinguish the separate species within each Q region [43]. Additionally, a broad hump was detected on the shielding side of Q^3 band in the spectra of pore solutions at ages between 1 day and 180 days, which is also observed in the spectra of concentrated alkali silicate solutions [42], representing polymerized Q^4 sites silicon. The asymmetrical shape of the hump indicates the incorporation of aluminum into the silicates [44,45], which agrees with the ^{27}Al NMR results. It is observed that the peak of the Q^4 band shifted in the direction of increased shielding from 7 days to 6 months and were less overlapping with the Q^3 band, which may be attributed to the decreasing amount of aluminum in the oligomers, as the ^{29}Si resonance frequency increases when the neighboring silicon is replaced by aluminum tetrahedra [46]. After 6 months, the Q^4 band became non-obvious indicating most of the aluminosilicate oligomers were condensed into geopolymer binders. The continuous condensation of the aluminosilicate oligomers observed here could further densify the microstructure of the geopolymer pastes after hardening, which supports the observations by other researchers [47,48] that the permeability of the fly ash geopolymer concrete reduced and the compressive strength increased from 90 d to 360 d. This can be a potential method (i.e., examining the ^{27}Al and ^{29}Si NMR spectra of the geopolymer pore solutions at ages) to determine the maturity of fly ash-based geopolymer. Further studies are necessary on this topic.

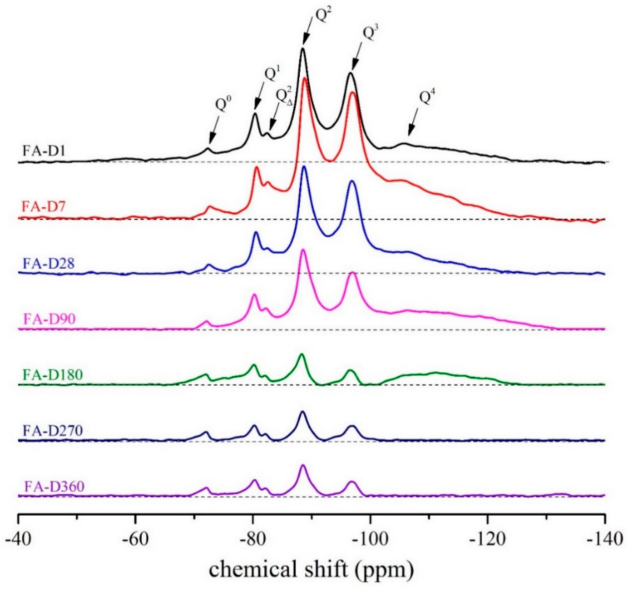

Figure 10. ^{29}Si NMR spectra of the geopolymer pore solutions at ages between 1 day and 1 year.

3.3. Relation of the Pore Solution to ASR Resistance of the Fly Ash Geopolymer

It has been reported that sufficient alkalinity in concrete pore solution is required to sustain the alkali-silica reaction at a certain rate that could lead to significant ASR expansion [15,20]. Several minimum hydroxide ion concentrations of pore solution have been proposed for deleterious expansion to occur in OPC concrete [14,27,49–51]. Several researchers [27,49,51] reported a minimum value of hydroxide ion concentration in pore solution between 0.2 to 0.3 mol/L under which deleterious ASR expansion is unlikely to occur, while Duchesne and Bérubé [50] proposed a relatively higher threshold

in hydroxide concentration around 0.65 mol/L and Struble [14] suggested a pH threshold between 13.65 and 13.83.

In the present study, the pH value of the pore solution in the fly ash geopolymer was stabilized at around 12.5, which is much lower than the thresholds proposed in the previous studies. Thus, the dissolution rate of the reactive silica in the pore solution here is unlikely to sustain the ASR due to the insufficient alkalinity of the pore solution, which most likely accounts for the low expansion of the geopolymer concrete prisms.

The carbonation of the pore solution in geopolymer is usually a concern that leads to the reduction of the pore solution alkalinity [52], while the infrared spectra in Figure 6 exhibit limited carbonation of the geopolymer pore solution in the present study, probably because the high humidity of the storage condition in concrete prism test largely inhibited the carbonation of the pore solution [53]. We thus concluded the rapid reduction of pH initially was mainly attributed to the consumption of the hydroxide ions for the fly ash dissolution. It should be noted that in a natural condition, carbonation of the geopolymer pore solution would happen [52] and further reduce its alkalinity, which could make fly ash geopolymer concrete even less vulnerable to ASR.

Pore solution of OPC concrete was mainly composed of highly concentrated alkali hydroxides with minor amounts of calcium hydroxides and sulfates [16,54]. In the studies of pore solution in OPC concrete, the hydroxide ion concentration was generally assumed to be equal to the concentration of alkali ions due to the electrical neutrality of the solution and other ionic species were insignificant in the solution compared to alkali ions [16,50]. Thus, concentration of alkali ions is often measured and used as an indication of the alkalinity of pore solution in OPC concrete. However, this assumption may not be applicable to the geopolymer pore solution, as both alkali ions and silicates were identified as the major components in the geopolymer pore solution and the silicates were the major anions balancing the alkali ions. Thus, high alkali content does not necessarily mean high hydroxide ion content or high pH value in the geopolymer pore solution. Using the alkali content to represent the pore solution alkalinity in the geopolymer system could be misleading and result in wrong interpretation of results.

It is known that the pore solution of normal OPC concrete is saturated with calcium hydroxides and the calcium content in the pore solution was typically ranged from 0.6 to 2.5 mmol/L [55] due to the low solubility of calcium hydroxides in the alkaline pore solution with pH level typically in a range of 13.2–13.8 [14]. The majority of calcium hydroxides from cement hydration are present in solid states in OPC. In the present study, the geopolymer synthesized by using the fly ash with calcium content of 1.2% is much lower compared to that in cement (62.5%). Despite the dissolution of fly ash lead to an increase of the calcium content up to 9.2 mmol/L at 7 days, the concentration is still much below the solubility of calcium hydroxides (~12 mmol/L [56]) in the pore solution with pH of 12.5. It indicates no soluble calcium source is available to further release calcium into the pore solution. With the condensation of the geopolymer, the calcium content is continued to reduce to 0.4 mmol/L, which is negligible when considering the effects of calcium on ASR expansions.

Calcium is believed to playing an important role on ASR expansion in OPC concrete. It has been reported that calcium could free up alkalis back into pore solution by exchanging the alkalis from ASR gels, which is known as "alkali recycling" [57,58]. Once the calcium in pore solution is consumed and incorporated into the gels, further dissolution of solid portlandite could compensate the deficiency of the calcium as well as hydroxide ions, to maintain the alkalinity in the pore solution. Thus, as the deficiency of calcium hydroxide acting as a "pH buffer" in geopolymer concrete, it can be reasonably expected that even though the ASR expansion occurs in the geopolymer concrete with sufficiently high alkalinity in the pore solution, the reaction cannot be sustained due to the consumption of hydroxide ions by ASR without compensating by calcium hydroxides.

Moreover, it has been suggested that calcium could facilitate the dissolution of reactive silica by promoting the gelation of silicates species in the pore solution to form poly-metal-silicates [17,18]. Thus, in addition to the insufficient alkalinity, the deficiency of calcium in the geopolymer pore solution

could also contribute to the reduction of the dissolution rate of the reactive silica and the gelation process might also be hindered due to the lack of polyvalent metal ions to link silica ions [59].

It has been reported that the presence of aluminate ions in the OPC pore solution contributed to mitigating the ASR expansion as the aluminum was incorporated into the silica structure on the aggregate surfaces, resulting in a reduction of the silica dissolution rate [21–23]. Chappex and Scrivener [22] showed that only 3.9 mmol/L aluminum in the pore solution was sufficient to significantly reduce the aggregate deterioration caused by ASR. In the OPC pore solution, which is mainly consisting of alkali hydroxide, the monomeric $Al(OH)_4^-$ should be the dominate aluminate phase [60]. In the current study, the infrared spectra (Figure 6) suggested the presence of Si-O-Al bonds in the pore solution and the ^{27}Al NMR spectra (Figure 9) further showed that all the aluminum tetrahedra within the pore solution were presented as q^4, q^3 and q^2 species in aluminosilicate oligomers. Despite the higher concentration of the aluminum in the fly ash geopolymer pore solution (Figure 5b), no monomeric $Al(OH)_4^-$ was present in the pore solution as the rapid condensation of the monomeric $Al(OH)_4^-$ with silicate species [60]. Further studies are necessary to reveal the influences of the presence of this type of aluminosilicate species in the pore solution on the ASR expansion of the fly ash-based geopolymer concrete.

4. Conclusions

This paper evaluated the ASR expansion behavior of the OPC and low-calcium fly ash-based geopolymer concrete containing alkali-silica reactive aggregates by using the concrete prism test. Pore solution analyses in terms of ion concentrations, pH, chemical bonds, and short-range order of the silicon and aluminum were conducted on the fly ash geopolymer paste at different ages up to one year.

The results showed that the pore solution of the low-calcium fly ash-based geopolymer in the current study was mainly composed of alkali ions, silicates, and aluminosilicates species, which is different from the pore solution in OPC concrete where high concentration of alkali hydroxides is the dominating component. Q^0-Q^4 sites silicon were detected in the geopolymer pore solution and all the aluminum in the pore solution were tetrahedrally coordinated, mainly present in the form of aluminosilicate oligomers. The condensation of the soluble species (e.g., aluminosilicate oligomers) in the pore solution into the geopolymer binder lasted almost for 6 months, after which the pore solution reached an equilibrium state.

The CPT results suggested much better ASR resistance of the fly ash geopolymer concrete compared to the OPC concrete. The lower expansion of the geopolymer concrete was most probably due to the insufficient alkalinity in the geopolymer pore solution in the present study. The pH of the pore solution reduced dramatically to 12.6 in only one day due to the consumption of hydroxide ions for the fly ash dissolution. Moreover, the deficiency of calcium and the presence of aluminum in the geopolymer pore solution might also contribute to enhancing the ASR resistance of geopolymer concrete. Further studies are necessary for better understanding of these effects on the ASR in the low-calcium fly ash-based geopolymer concrete.

Author Contributions: Conceptualization, E.-H.Y. and J.L.; methodology, J.L.; validation, J.F. and J.L.; formal analysis, J.L. and J.F.; investigation, J.F. and J.L.; writing—original draft preparation, J.L.; writing—review and editing, E.-H.Y.; supervision, E.-H.Y.; project administration, E.-H.Y.; funding acquisition, E.-H.Y. All authors have read and agreed to the published version of the manuscript.

Funding: This research was funded by JTC (M4061754 JTC-Yang En-Hua).

Conflicts of Interest: The authors declare no conflict of interest.

References

1. Stanton, T. Expansion of concrete through reaction between cement and aggregate. In Proceedings of the American Society of Civil Engineers, Reston, VA, USA, December 1940; Volume 66, pp. 1781–1811.

2. Fournier, B.; Bérubé, M.-A. Alkali-aggregate reaction in concrete: A review of basic concepts and engineering implications. *Can. J. Civ. Eng.* **2000**, *27*, 167–191. [CrossRef]
3. Diamond, S. A review of alkali-silica reaction and expansion mechanisms 1. Alkalies in cements and in concrete pore solutions. *Cem. Concr. Res.* **1975**, *5*, 329–345. [CrossRef]
4. Rajabipour, F.; Giannini, E.; Dunant, C.F.; Ideker, J.H.; Thomas, M.D. Alkali–silica reaction: Current understanding of the reaction mechanisms and the knowledge gaps. *Cem. Concr. Res.* **2015**, *76*, 130–146. [CrossRef]
5. Wright, J.R.; Shafaatian, S.; Rajabipour, F. Reliability of chemical index model in determining fly ash effectiveness against alkali-silica reaction induced by highly reactive glass aggregates. *Constr. Build. Mater.* **2014**, *64*, 166–171. [CrossRef]
6. Thomas, M. The effect of supplementary cementing materials on alkali-silica reaction: A review. *Cem. Concr. Res.* **2011**, *41*, 1224–1231. [CrossRef]
7. Wallah, S.E.; Rangan, B.V. *Low-Calcium Fly Ash-based Geopolymer Concrete: Long-term Properties*; Curtin University of Technology: Perth, WA, Australia, 2006; Available online: http://hdl.handle.net/20.500.11937/34322.
8. Bernal, S.A.; Provis, J.L. Durability of Alkali-Activated Materials: Progress and Perspectives. *J. Am. Ceram. Soc.* **2014**, *97*, 997–1008. [CrossRef]
9. Li, C.; Sun, H.; Li, L. A review: The comparison between alkali-activated slag (Si+Ca) and metakaolin (Si+Al) cements. *Cem. Concr. Res.* **2010**, *40*, 1341–1349. [CrossRef]
10. Xie, Z.; Xiang, W.; Xi, Y. ASR Potentials of Glass Aggregates in Water-Glass Activated Fly Ash and Portland Cement Mortars. *J. Mater. Civ. Eng.* **2003**, *15*, 67–74. [CrossRef]
11. Fernández-Jiménez, A.; García-Lodeiro, I.; Palomo, A. Durability of alkali-activated fly ash cementitious materials. *J. Mater. Sci.* **2007**, *42*, 3055–3065. [CrossRef]
12. García-Lodeiro, I.; Palomo, A.Y.; Fernández-Jiménez, A. Alkali–aggregate reaction in activated fly ash systems. *Cem. Concr. Res.* **2007**, *37*, 175–183. [CrossRef]
13. Kupwade-Patil, K.; Allouche, E. Impact of Alkali Silica Reaction on Fly Ash-Based Geopolymer Concrete. *J. Mater. Civ. Eng.* **2013**, *25*, 131–139. [CrossRef]
14. Struble, L.J. The Influence of Cement Pore Solution on Alkali-Silica Reaction. Ph.D. Thesis, Purdue University, West Lafayette, Indiana, May 1987.
15. Shehata, M.H.; Thomas, M.D. Alkali release characteristics of blended cements. *Cem. Concr. Res.* **2006**, *36*, 1166–1175. [CrossRef]
16. Swamy, R.N. *The Alkali-Silica Reaction in Concrete*; CRC Press: London, UK, 1992.
17. Glasser, L.D.; Kataoka, N. On the role of calcium in the alkali-aggregate reaction. *Cem. Concr. Res.* **1982**, *12*, 321–331. [CrossRef]
18. Gaboriaud, F.; Nonat, A.; Chaumont, D.; Craievich, A. Aggregation and Gel Formation in Basic Silico−Calco −Alkaline Solutions Studied: A SAXS, SANS, and ELS Study. *J. Phys. Chem. B* **1999**, *103*, 5775–5781. [CrossRef]
19. Bleszynski, R.F.; Thomas, M.D. Microstructural Studies of Alkali-Silica Reaction in Fly Ash Concrete Immersed in Alkaline Solutions. *Adv. Cem. Based Mater.* **1998**, *7*, 66–78. [CrossRef]
20. Vayghan, A.G.; Rajabipour, F.; Rosenberger, J.L. Composition–rheology relationships in alkali–silica reaction gels and the impact on the gel's deleterious behavior. *Cem. Concr. Res.* **2016**, *83*, 45–56. [CrossRef]
21. Leemann, A.; Bernard, L.; Alahrache, S.; Winnefeld, F. ASR prevention—Effect of aluminum and lithium ions on the reaction products. *Cem. Concr. Res.* **2015**, *76*, 192–201. [CrossRef]
22. Chappex, T.; Scrivener, K.L. The influence of aluminium on the dissolution of amorphous silica and its relation to alkali silica reaction. *Cem. Concr. Res.* **2012**, *42*, 1645–1649. [CrossRef]
23. Warner, S.J. The role of alumina in the mitigation of alkali-silica reaction. Master's Thesis, Oregon State University, Corvallis, Oregon, March 2012.
24. ASTM Committee C09.26, ASTM C1260-14. *Standard Test Method for Potential Alkali Reactivity of Aggregates (Mortar-Bar Method)*; ASTM Int.: West Conshohocken, PA, USA, 2014; pp. 1–5. [CrossRef]
25. Nguyen, A.D.; Škvára, F. The influence of ambient pH on fly ash-based geopolymer. *Cem. Concr. Compos.* **2016**, *72*, 275–283. [CrossRef]
26. ASTM C1293-08b (2015). *Standard Test Method for Determination of Length Change of Concrete Due to Alkali-Silica Reaction*; ASTM Int.: West Conshohocken, PA, USA, 2015.

27. Thomas, M.; Fournier, B.; Folliard, K.; Ideker, J.; Shehata, M. Test methods for evaluating preventive measures for controlling expansion due to alkali–silica reaction in concrete. *Cem. Concr. Res.* **2006**, *36*, 1842–1856. [CrossRef]
28. Lahoti, M.; Wong, K.K.; Tan, K.H.; Yang, E.-H. Use of alkali-silica reactive sedimentary rock powder as a resource to produce high strength geopolymer binder. *Constr. Build. Mater.* **2017**, *155*, 381–388. [CrossRef]
29. Barneyback, R.; Diamond, S. Expression and analysis of pore fluids from hardened cement pastes and mortars. *Cem. Concr. Res.* **1981**, *11*, 279–285. [CrossRef]
30. Cyr, M.; Rivard, P.; Labrecque, F.; Daidié, A. High-Pressure Device for Fluid Extraction from Porous Materials: Application to Cement-Based Materials. *J. Am. Ceram. Soc.* **2008**, *91*, 2653–2658. [CrossRef]
31. Hou, X.; Kirkpatrick, R.J.; Struble, L.J.; Monteiro, P.J.M. Structural Investigations of Alkali Silicate Gels. *J. Am. Ceram. Soc.* **2005**, *88*, 943–949. [CrossRef]
32. Duxson, P.; Lukey, G.C.; Separovic, F.; Van Deventer, J.S.J. Effect of Alkali Cations on Aluminum Incorporation in Geopolymeric Gels. *Ind. Eng. Chem. Res.* **2005**, *44*, 832–839. [CrossRef]
33. Buchwald, A.; Zellmann, H.-D.; Kaps, C. Condensation of aluminosilicate gels—model system for geopolymer binders. *J. Non-Cryst. Solids* **2011**, *357*, 1376–1382. [CrossRef]
34. Bernal, S.A.; De Gutierrez, R.M.; Provis, J.L.; Rose, V. Effect of silicate modulus and metakaolin incorporation on the carbonation of alkali silicate-activated slags. *Cem. Concr. Res.* **2010**, *40*, 898–907. [CrossRef]
35. Ruiz-Trejo, E.; Zhou, Y.; Brandon, N.P. On the manufacture of silver-$BaCe_{0.5}Zr_{0.3}Y_{0.16}Zn_{0.04}O_3-\delta$ composites for hydrogen separation membranes. *Int. J. Hydrog. Energy* **2015**, *40*, 4146–4153. [CrossRef]
36. Martineau-Corcos, C.; Taulelle, F.; Haouas, M. *The Use of 27Al NMR to Study Aluminum Compounds: A Survey of the Last 25 Years*; Wiley: Hoboken, NJ, USA, 2016; pp. 1–51.
37. Lippmaa, E.; Samoson, A.; Magi, M. High-resolution aluminum-27 NMR of aluminosilicates. *J. Am. Chem. Soc.* **1986**, *108*, 1730–1735. [CrossRef]
38. Samadi-Maybodi, A.; Azizi, S.N.; Naderi-Manesh, H.; Bijanzadeh, H.; McKeag, I.H.; Harris, R.K. Highly resolved 27Al NMR spectra of aluminosilicate solutions. *J. Chem. Soc. Dalton Trans.* **2001**, 633–638. [CrossRef]
39. Azizi, S.N.; Ehsani-Tilami, S. Theoretical and Experimental27Al NMR Chemical Shift Studies on End-Group Aluminates Linked to Different Silicate Species. *J. Chin. Chem. Soc.* **2009**, *56*, 898–907. [CrossRef]
40. Engelhardt, G.; Fahlke, B.; Magi, M.; Lippmaa, E. High-resolution solid-state 29Si and 27Al n.m.r. of aluminosilicate intermediates in zeolite A synthesis. *Zeolites* **1983**, *3*, 292–294. [CrossRef]
41. Glasser, L.S.D.; Harvey, G. The unexpected behaviour of potassium aluminosilicate solutions. *J. Chem. Soc. Chem. Commun.* **1984**, 664–665. [CrossRef]
42. Bass, J.L.; Turner, G.L. Anion Distributions in Sodium Silicate Solutions. Characterization by29SI NMR and Infrared Spectroscopies, and Vapor Phase Osmometry. *J. Phys. Chem. B* **1997**, *101*, 10638–10644. [CrossRef]
43. Phair, J.; Van Deventer, J. Effect of the silicate activator pH on the microstructural characteristics of waste-based geopolymers. *Int. J. Miner. Process.* **2002**, *66*, 121–143. [CrossRef]
44. Lippmaa, E.; Maegi, M.; Samoson, A.; Tarmak, M.; Engelhardt, G. Investigation of the structure of zeolites by solid-state high-resolution silicon-29 NMR spectroscopy. *J. Am. Chem. Soc.* **1981**, *103*, 4992–4996. [CrossRef]
45. Brus, J.; Abbrent, S.; Kobera, L.; Urbanova, M.; Cuba, P. *Advances in 27Al MAS NMR Studies of Geopolymers*; Elsevier BV: Amsterdam, The Netherlands, 2016; pp. 79–147.
46. Kinrade, S.D.; Swaddle, T.W. Direct detection of aluminosilicate species in aqueous solution by silicon-29 and aluminum-27 NMR spectroscopy. *Inorg. Chem.* **1989**, *28*, 1952–1954. [CrossRef]
47. Gunasekara, C.; Law, D.W.; Setunge, S. Long term permeation properties of different fly ash geopolymer concretes. *Constr. Build. Mater.* **2016**, *124*, 352–362. [CrossRef]
48. Wardhono, A. The Durability of Fly ash Geopolymer and Alkali-activated Slag Concretes. Ph.D. Thesis, RMIT University, Melbourne, Australia, 2014.
49. Diamond, S. Alkali reactions in concrete-pore solution effects. In Proceedings of the 6th International Conference on Alkali-Aggregate Reaction in Concrete, Copenhagen, Denmark, 1983; pp. 155–166.
50. Duchesne, J.; Berube, M. The effectiveness of supplementary cementing materials in suppressing expansion due to ASR: Another look at the reaction mechanisms part 2: Pore solution chemistry. *Cem. Concr. Res.* **1994**, *24*, 221–230. [CrossRef]
51. Kollek, J.J.J.; Varma, S.P.P.; Zaris, C. Measurement of OH- Ion Concentrations of Pore Fluids and Expansion Due to Alkali-Silica Reaction in Composite Cement Mortars. In Proceedings of the 8th International Congress on the Chemistry of Cement, Rio de Janeiro, Brazil, 1986; Volume 4, pp. 183–189.

52. Pouhet, R.; Cyr, M. Carbonation in the pore solution of metakaolin-based geopolymer. *Cem. Concr. Res.* **2016**, *88*, 227–235. [CrossRef]
53. Saetta, A.V.; Schrefler, B.A.; Vitaliani, R.V. The carbonation of concrete and the mechanism of moisture, heat and carbon dioxide flow through porous materials. *Cem. Concr. Res.* **1993**, *23*, 761–772. [CrossRef]
54. Diamond, S. ASR-another look at mechanisms. In Proceedings of the 8th International Conference Alkali-Aggregate React, Kyoto, Japan, 1989; pp. 83–94.
55. Helmuth, R.; Stark, D.; Diamond, S.; Moranville-regourd, M. *Alkali-Silica Reactivity: An Overview of Research*; Strategic Highway Research Program: Washington, DC, USA, 1993.
56. Yuan, T.; Wang, J.; Li, Z. Measurement and modelling of solubility for calcium sulfate dihydrate and calcium hydroxide in NaOH/KOH solutions. *Fluid Phase Equilib.* **2010**, *297*, 129–137. [CrossRef]
57. Hanson, W.C. Studies relating to the mechanism by which the alkali-aggregate reaction produces expansion in concrete. *ACI J. Proc.* **1944**, *40*, 213–228. [CrossRef]
58. Thomas, M. The role of calcium hydroxide in alkali recycling in concrete. *Mater. Sci. Concr. Spec.* **2001**, 225–236.
59. Glasser, L. The chemistry of silica. *Endeavour* **1980**, *4*, 126. [CrossRef]
60. Sagoe-Crentsil, K.; Weng, L. Dissolution processes, hydrolysis and condensation reactions during geopolymer synthesis: Part II. High Si/Al ratio systems. *J. Mater. Sci.* **2006**, *42*, 3007–3014. [CrossRef]